International Journal of Mechanical and Production Engineering Research and Development (IJMPERD)
ISSN (P): 2249-6890; ISSN (E): 2249-8001
Vol. 8, Issue 4, Aug 2018, 653-666

ANALYSIS OF PIN-FIN GEOMETRY EFFECT ON MICROCHANNEL HEAT SINK PERFORMANCE

SUBHASH V. JADHAV, PRASHANT M. PAWAR & BABRUVAHAN P. RONGE

SVERI's College of Engineering, Pandharpur, Maharashtra, India

ABSTRACT

Purpose

The effect of pin fin geometry on the thermal performance of a microchannel heat sink is numerically analyzed in this study.

Design/Methodology/Approach

A numerical analysis is carried out using the conjugate heat transfer module of COMSOL MULTIPHYSICS software. The performance of microchannel is presented in terms of Nusselt number and pressure drop. Initially, the baseline model of a microchannel with elliptical pin fins is validated with results from the literature. The different shapes of pin fin are compared for their performance. In the later part of the paper, the effect of the change in elliptic pin fin orientation in the channel, different pin fin height and different axial distance between fins, is analyzed.

Findings

The thermal performance of a microchannel with square pin fins is found to be better, while the elliptical pin fin shows a minimum pressure drop. The 40^{o} angle of the major axis of the elliptic pin fin with the channel axis is found to give better performance than other angles. Elliptical pin fins with 700µm pin fin height and 1300µm axial distance between fins in the microchannel performed better than other values. Increasing the pin fin height and proper selection of axial distance between fins are found to be better methods of increasing microchannel performance.

Originality/Value

This study is helpful in proper selection of pin fin geometry for enhancing the performance of microchannel heat sink.

KEYWORDS: Microchannel Heat Sink, Nusselt Number, Pressure Drop, Fin Shapes & Fin Height

Received: Jun 17, 2018; **Accepted**: Jul 08, 2018; **Published**: Jul 20, 2018; **Paper Id.**: IJMPERDAUG201868

Original Article

INTRODUCTION

The previous century witnessed the miniaturization of modern electronic components. Heats dissipated by these modern compact and sophisticated microelectronic components have increased drastically. Corresponding high operating temperature values threaten the proper functioning of these components and have resulted in a lot of research being carried out for enhancing heat transfer technologies. Though there are a lot of technologies being researched, microchannel heat sinks with higher heat transfer capabilities are considered to be one of the most promising solutions to this problem. Also, with the availability of modern advanced micro fabrication technologies, it is now possible to integrate the microchannels directly on the base of the heat generating substrate of these

electronic components, making it possible to use this technology in microelectronic cooling applications. Tuckerman and pees in (1981) initially proposed the use of micro channels for electronic cooling applications. Many passive and active heat transfer enhancement techniques are also being tested for this purpose.

Cheng, Y. J. (2007) observed that the stacked micro channel having passive structures perform better than smooth microchannel. Jinliang et al. (2010) in his study concluded that the periodic thermal developing flow is responsible for heat transfer enhancement. John et al. (2010) observed that at low Reynolds number, the heat sinks with circular pin-fins shows better performance compared with heat sinks having square pin-fins and vice versa. Minghou et al. (2011) experimentally analyzed pressure drop and average Nusselt number and developed correlation for the same. Monoj et al. (2011) observed that in a staggered arrangement, the perforated elliptical pin fins perform better than the solid elliptic pin fins. Carlos et al. (2013) concluded that the heat sink having offset micro pin fin is a good option for cooling the IC chips. Tullius et al. (2012) numerically investigated the effect of fin shapes in minichannels and found that the optimal shape of fins is dependent on the fluid flow rate through the channel. Chiu et al. (2013) numerically studied the heat transfer in heat sinks with micro-pin-fins with different longitudinal spacing and transverse spacing. Haleh et al. (2013) observed that the heat sinks could be optimized using entropy generation minimization. Saad A. J. et al. (2014) experimentally investigated geometrically enhanced heat sinks by using water and concluded that water still has a lot of potential to cool the high heat generating microprocessors. Tzer et al. (2015) observed that the Nusselt number depends on center-to-center transverse distance and is independent of the center-to-center longitudinal distance between pin fins. A semi-empirical correlation was developed by Hafiz M. A. and Adrian B. (2015) to account for the combined effect of gravity and surface tension and the results obtained were found to be in good agreement with experimental data. Türker et al. (2015) numerically studied heat transfer and hydraulic performance of a single micro pin-fin, with the same diameters and different shapes. Jin et al. (2016) in his numerical studies concluded that a reasonable heat transfer could be achieved by locating a rectangular pin fin in a microchannel heat sink. Kirsch et al. (2017) investigated microchannel pin fin arrays that were manufactured using Laser Powder Bed Fusion over a range of Reynolds numbers to study the pressure loss and heat transfer capability. Microprocessor cooling with Nanofluids was investigated by Aysha M. S. et. al. (2017) and concluded that with the increase in Reynolds number, Cu-water nanofluid showed better trends of thermal enhancement than Al2O3-water nanofluid.

Selection of fluid type and its flow velocities, choice of material for heat sink and with different channel surface modifications, are some of the areas related to a heat sink where research is being undertaken. It is observed by many researchers that using fins in microchannel enhances its thermal performance and the research in this area mostly focused on pin fins of different shapes. Many researchers have reported that the elliptical pin fins exhibit poor thermal performance. But the pressure drop offered by the elliptical pin fins is minimum, among the different pin fin shapes considered. Since the thermal performance of elliptical pin fin is poor, further investigation has not been done related to microchannels with elliptical pin fins. Therefore there is a need for further detail investigation of microchannels with elliptical fins and different methods to further enhance the thermal performance of elliptical pin fins, along with its lower pressure drop advantage. The prime focus of this study is to numerically analyze a microchannel heat sink with different orientations and heights of elliptical pin fins so that their thermal performance can be enhanced.

DESCRIPTION OF PHYSICAL MODEL

Microchannel Heat Sink

All the microchannels in the heat sink considered for this study, are geometrically identical. Therefore to reduce computational time, a single element of microchannel heat sink with fluid in it, is considered as a computational domain, instead of the complete heat sink. Schematic of a microchannel used in the present study is as shown in (Figure 1). A uniform heat flux is applied to the channel base, from its bottom side. Length of the channel (L) used for the analysis is 15mm. Wall thickness (t) of the microchannel is 100 µm. The flow cross-sectional area of the channel is 1000µm X 1000 µm. The channel width (W) and height (H) are 1200µm each. Copper is used as heat sink material due to its higher thermal conductivity and lower thermal resistance. The coolant used in this study is water.

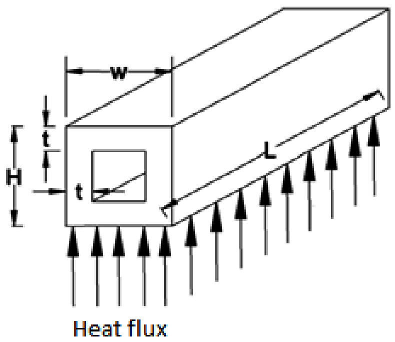

Figure 1: Schematic of the Heat Sink Unit Cell used for the Analysis

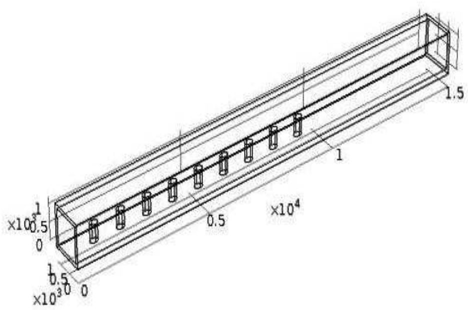

Figure 2: Baseline Model used in the Study

To simplify the problem, the following assumptions are considered during the numerical analysis.

- The flow is steady and laminar.
- Coolant fluid used is incompressible.
- No slip boundary conditions are assumed at the walls.
- Fluid enters the channel with uniform velocity.
- The properties of both the fluid and solid are temperature independent.
- Radiation heat transfer is neglected.

The following Continuity equation, Conservation of momentum and Conservation of energy [Equations (1) - (4)] are used to describe the fluid flow and heat transfer in this analysis.

$$\nabla U = 0 \tag{1}$$

$$\rho(U \cdot \nabla U) + \Delta P - \mu\nabla^{2} T = 0 \tag{2}$$

$$U.\nabla T = 0 \text{ (for solids)} \tag{3}$$

$$\rho Cp(U . \nabla T) - k_f(\nabla^{2} T) = 0 \text{ (for fluid)} \tag{4}$$

The performance parameters used in this study for analyzing the microchannel performance are the Nusselt number, Reynolds number, Pressure drop and Fanning friction factor. The Reynolds number depends on the fluid density (ρ), Average axial velocity (u), the hydraulic diameter of the channel (Dc), over the dynamic viscosity (μ). The values of average axial velocity in the channel are obtained from simulation results.

$$Re = \frac{\rho u\, Dc}{\mu} \tag{5}$$

Nu is can be calculated using average heat transfer coefficient (h), the hydraulic diameter of the channel (Dc), and the thermal conductivity (k). The value of heat transfer coefficient (h) is obtained from simulations. The Fanning friction factor (f) is derived from Kakac et al. (1987), as shown in Equation (7).

$$Nu = \frac{hDc}{k} \tag{6}$$

$$\text{f. Re} = 14.23 \tag{7}$$

NUMERICAL ANALYSIS OF BASELINE MODEL

For predicting the behavior of the heat transfer process in the microchannel heat sink, a three-dimensional representative control volume of the microchannel is used as a baseline model in this analysis and is as shown in (Figure 2). Nine elliptical pin fins of 500µm height are located in the channel at 1000µm apart, along the channel base centerline. The Major axis and minor axis of the elliptical pin fin are 150µm and 100µm respectively. Heat flux is applied at the channel base. The heat entering into channel base is transferred to channel walls by conduction and further to the coolant fluid by convection. Therefore, this is a conjugative heat transfer problem. Considering this, the conjugative heat transfer module of COMSOL MULTIPHYSICS software is used for the analysis. The value of heat flux applied at the channel base is $20W/cm^2K$. The coolant inflow velocity is varied from 0.2 m/s to 1m/s. The thermal conductivity of the coolant used for the analysis is 0.608W/m K and density is $1000kg/m^2$.

The boundary conditions applied to the control volume, in the present analysis, is as shown in Table 1. Water at 293.15K enters the channel with uniform velocity and flows further through the channel with no slip boundary condition. The flow is assumed to be fully developed at the outlet. Atmospheric pressure is assigned at the fluid outlet boundary of the channel. Appropriate values of thermophysical properties are assigned for the solid and fluid regions. The heat received by the channel base is further conducted to the channel walls. This heat is then transferred by convection to the fluid in the channel. The solid liquid boundaries in the channel are assigned with no slip boundary condition.

Table 1: Boundary Conditions used for the Analysis

Boundary	Fluid Boundary Condition	Thermal Boundary Condition
Front inlet	Inlet	Adiabatic
Front solid	Wall	Adiabatic
Right	Symmetry	Symmetry
Top	Wall	Adiabatic
Left	Symmetry	Symmetry
Bottom	Wall	Uniform heat flux
Back outlet	Outlet	Adiabatic
Back solid	Wall	Adiabatic

In order to check the sensitivity of the numerical results to the mesh size, the grid independency for the baseline model was checked for five different grid sets as shown in the (Table 2). The values of the channel outlet temperature and average velocity in the channel obtained after simulation runs are as shown in (Figure 3) and (Figure 4) respectively. From the figure, it can be observed that after the fourth set of simulation, further increasing the grid have a negligible effect on the results. The error observed in the values of outlet temperature and average velocity is less than 0.8%.

The baseline model is validated by comparing its simulation results with the results obtained by Tullius et al. [8], under similar conditions. The comparison for the variation of the Nusselt number versus Reynolds number is as shown in (Figure 4). It can be observed from the figure that, the present baseline model results are in good agreement with that of results of Tullius et al. Therefore the conditions of the fourth case are used for further, for all simulations in this study.

Table 2: Grid Independency Test

Sr. No. of Simulation Run	1	2	3	4	5
Tetrahedral Elements	22243	57906	95754	211131	437675
Average Element quality	0.6075	0.6632	0.6885	0.7206	0.7297
Average Growth Rate	1.957	1.802	1.748	1.694	1.695

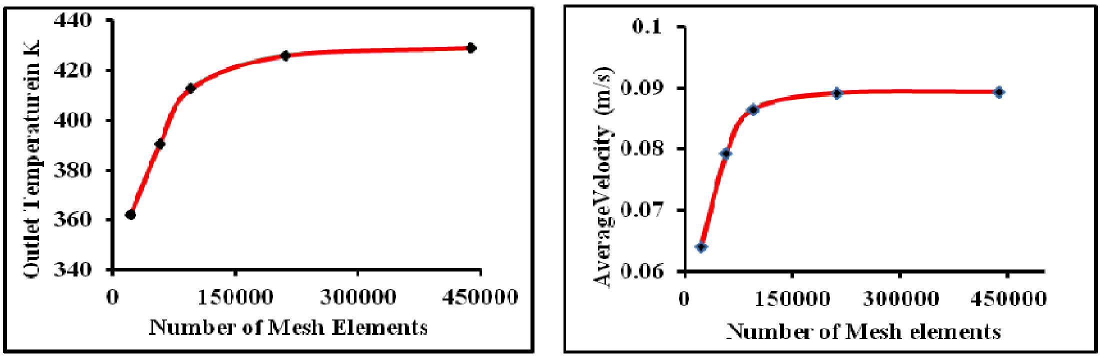

Figure 3: Mesh Independency Study with Different Mesh Elements.
(a) Outlet Temperature Versus Number of Mesh Elements
(b)Average Velocity in Channel Versus Number of Mesh Elements

RESULTS AND DISCUSSIONS

Analysis of Microchannel with Different Pin Fin Shapes

This study is done to understand how the different parameters related to pin fins located on the channel base, effects the thermal performance of the heat sink. In order to enhance the heat transfer performance of a microchannel heat sink, generally the methods adopted are, either to increase the heat transfer area or increase the heat transfer coefficient.

Changing the shape generally changes the heat transfer area. Therefore to understand properly the effect of shape, in this study the validated microchannel from the previous section is used for further analysis, keeping the contact surface area between the coolant and microchannel constant. The different microchannels are designed for the same contact surface area. In order to do this, the surface area of the fin is kept constant, while changing the fin shape. Moreover, for all the fin shapes, the height considered is 500µm in the first part of the study. Thus, whatever change in performance, can be solely attributed to fin shape. The four different pin fins shapes considered in this study are ellipse, circle, hexagon, and square.

The variation of pressure drop with Reynolds number and Nusselt number with Reynolds number for the microchannel with different pin fin shapes is as shown in [(Figure 5) and (Figure 6)]. The pressure drop for elliptical pin fin is observed to be minimum and for circular pin fin, it is maximum. The unobstructed flow between the row of fins and the microchannel wall is maximum in case of elliptical fins. Since more fluid is able to flow without obstruction, the pressure drop in the channel is minimum with elliptical fins as seen in (Figure 8d). Similarly, the unobstructed flow is minimum in case of circular fins. Thus, due to higher obstruction for the fluid flow due to fins, the pressure drop is maximum in case of circular fins as shown in (Figure 8c). The obstruction for the fluid flow, for the remaining two shapes, is in between that of elliptical and circular fins. Therefore the pressure drop for square and hexagonal fins is also in between that of elliptical and circular fins.

As shown in (Figure 8a) the flow separation is maximum with square pin fins. This flow separation due to the row of square fins results in maximum disturbance of the thermal boundary layer and corresponding mixing near the walls, enhancing the heat transfer from channel walls to the fluid. The elliptical fins are observed to have minimum flow separation as well as boundary layer disturbance. But with elliptical fins, the heat transfer from the fins to the liquid will be comparatively more since the fluid is having more contact with the fins while flowing smoothly around the fins. on the other hand, hexagonal fins have both heat transfer from walls as well as from the fins to be lesser comparatively. Wall heat transfer is less due to lesser boundary layer disturbance. while the heat transfer from fin is less due to lesser contact between fluid and fins when the fluid is flowing around it. This results in a lesser Nusselt number with the hexagonal fins when compared to other shapes.

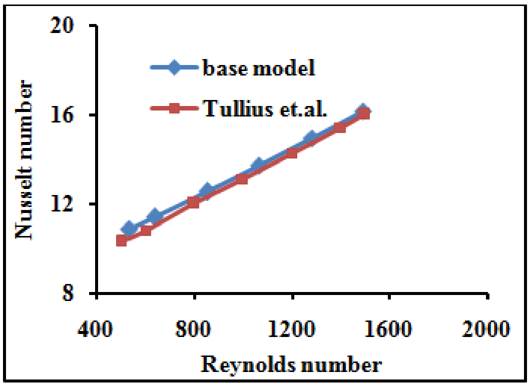

Figure 4: Validation of Basic Model with Results from Tullius et al. [8]

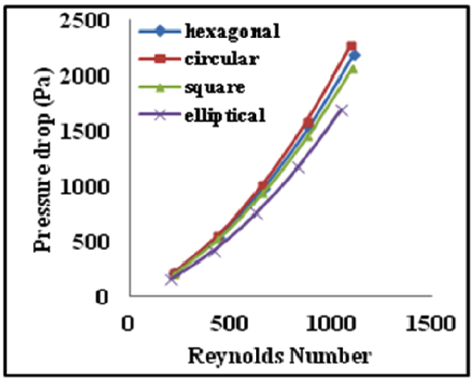

Figure 5: Variation of Pressure Drop with Reynolds Number

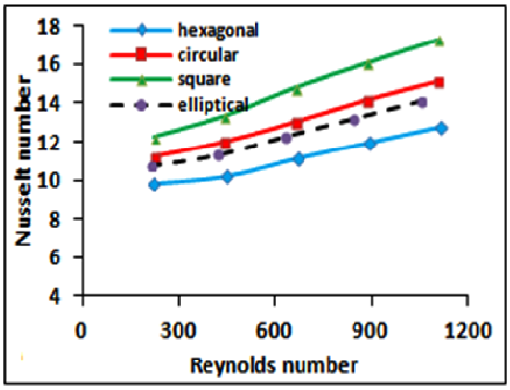

Figure 6: Variation of Nusselt Number with Reynolds Number

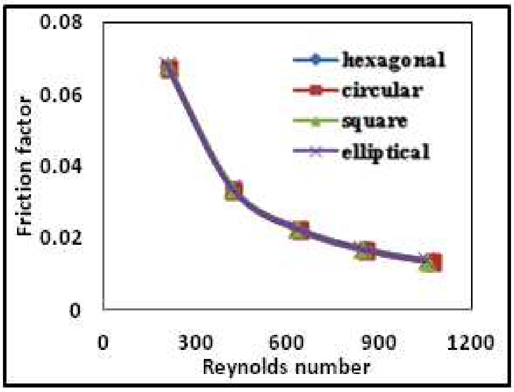

Figure 7: The Variation of Friction Factor with Reynolds Number

Therefore, it can be observed that elliptical fins offer minimum pressure drop while, their heat transfer capability is also comparatively higher, though not the highest. One of the major reason for the minimum pressure drop with elliptical fins is its orientation in the microchannel with the major axis of the elliptical fin parallel to the channel axis. This orientation of the fins in the channel results in minimum flow obstruction and therefore the pressure drop is minimum with elliptical fins. Considering the above facts, in the next section, the orientation of the pin fins is varied to understand its effect.

The variation of Fanning friction factor with Reynolds number is as shown in (Figure 7). It can be observed that the Fanning friction factor curve remains similar for all pin fin shapes. The Fanning friction factor is a function of pressure loss resulting from wall friction. Since the surface area considered in all cases is the same, the wall friction remains the same which results in obtaining a similar curve for all cases, throughout this study.

Analysis of Microchannel with Elliptical Pin Fins of Different Height

In this section, further study is done to analyze the effect of the height of the elliptical pin fin on the microchannel performance. The pin fin height is varied from 300μm to 700μm. The surface area of the pin fin is kept constant while designing these microchannels. The curves for the variation of pressure drop with Reynolds number is as shown in (Figure 9). The pressure drop is observed to increase with the height of the fins. With the increase in pin fin height, the obstruction for the fluid flow increases, thereby resulting in a higher pressure drop. The least pressure drop is observed with 300μm pin height, while the 700μm pin fin height exhibits maximum pressure drop.

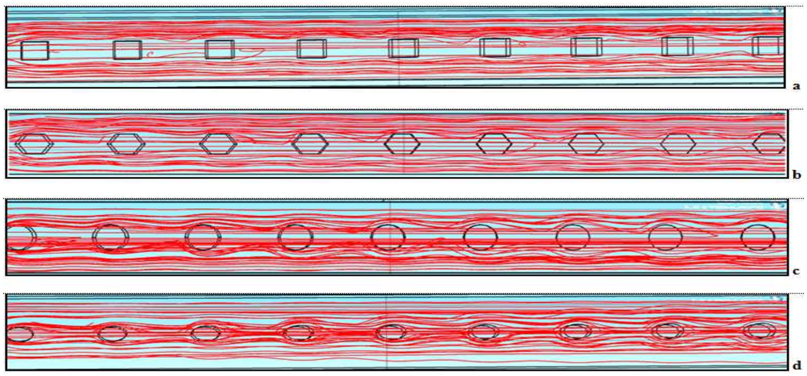

Figure 8: Streamlines for Different Fin Shapes a) Square b) Hexagonal c) Circular d) Elliptical

The variation of Nusselt number with Reynolds number is as shown in (Figure 10). It is observed from the figure that with increasing pin fin height, thermal performance of the microchannel increases. The increment in the Nusselt number can be attributed to the increased flow separation, flow reversals, disturbance of thermal boundary layer due to mixing, etc. The fluid flow separation happening due to the row of fins located along the microchannel axis increases with an increase in the height of the pin fin. The higher amount of flow separation with height, results in higher mixing in the boundary layer, thereby increasing the convective heat transfer. Thus, as the pin fin height increases, the thermal performance of the microchannel also increases. (Figure 11) shows the pressure drop happening in the microchannels with 0.2m/s fluid inlet velocity. It is clear from the figure that, the cross section of shorter fins is wider and that of longer fins is comparatively narrow.

The minimum and maximum increment in pressure drop and Nusselt number for a microchannel with elliptical pin fin of heights ranging from 300µm to 700µm are as shown in (Table 3). The least Nusselt number value is observed with 300µm, while maximum with 700µm. The maximum increment of 26.4% in Nusselt number is observed with 700µm elliptical pin fin. An increment of 45.5% between the minimum and maximum values of Nusselt number values is observed in this study. From (Figure 12), It can be clearly observed that the Nusselt number increases with inlet velocity for all pin fin heights.

Analysis of Microchannel with Elliptical Pin Fins with Different Orientation

In this section, an analysis is done for microchannels with elliptical pin fins. The pin fin orientation in the microchannel is varied to understand its effect. The validated microchannel baseline model from the previous section is used here for further analysis. In the baseline model, the major axis of the ellipse was oriented along the flow direction i.e. parallel to the channel axis. The angle made by the major axis of the ellipse is varied from ten degrees (10^o) to ninety degrees (90^o), in steps of ten degrees. The height of the fin used for the simulation is 500µm. The variation of Pressure drop in the microchannel with Reynolds number is as shown in (Figure 13). From the figure, it can be observed that the pressure drop in the channel correspondingly increases, as the angle is increased from ten degrees to ninety degrees. This increment in pressure drop can be clearly attributed to increased flow obstruction due to changed pin fin orientation. The pressure drop increment is less for lower values of Reynolds number and increases with the increase in Reynolds number.

The variation of Nusselt number with Reynolds number for different pin fin orientation is as shown in (Figure 15). It can be observed that, for 40^o angle of elliptic pin fin in the microchannel, the Nusselt number obtained is maximum. The value of Nusselt number for lower and higher values of angle is observed to be comparatively lower. Thus the best value of Nusselt number observed is 40^o angle.

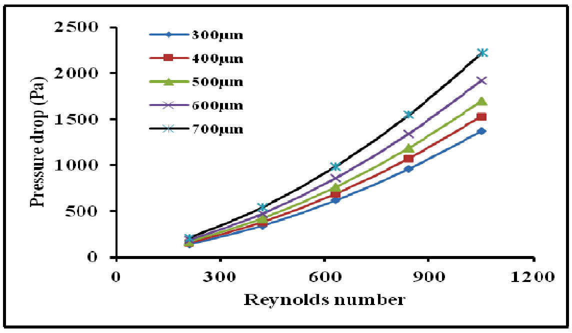

Figure 9: Variation of Pressure Drop with Reynolds Number

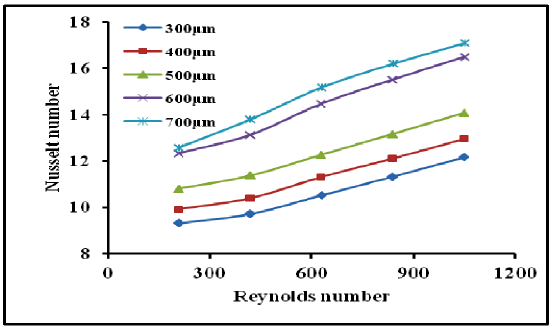

Figure 10: Variation of Nusselt number with Reynolds NUMBER

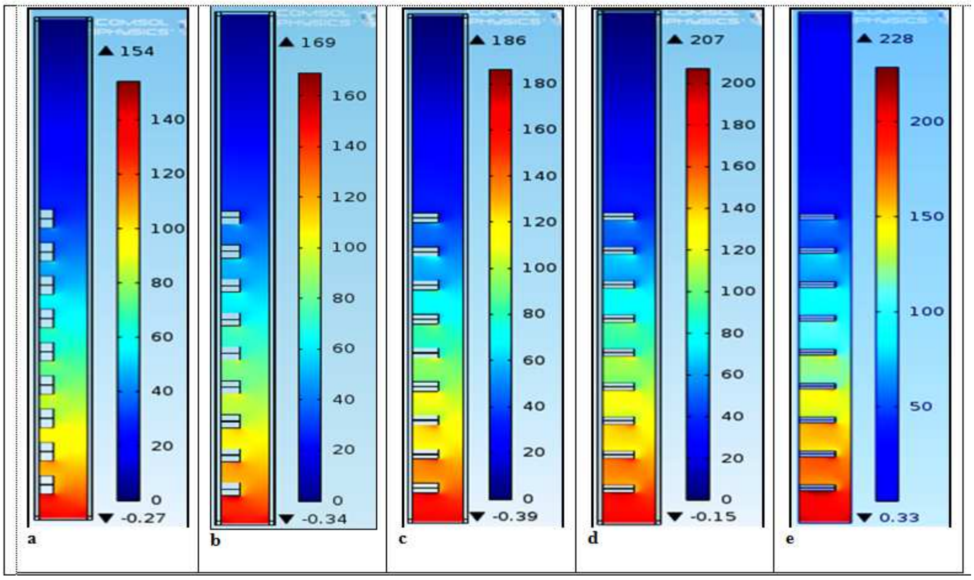

Figure 11: Pressure Variation for Different fin Height a)300µm b)400µm c)500µm d)600µm e)700µm

Table 3: Percentage Increment in Pressure Drop and Nusselt Number in Different Microchannels

Pin Fin Height (µm)	Maximum ΔP (Pa)	Minimum ΔP (Pa)	% Increment in ΔP (Pa)	Maximum Nu	Minimum Nu	% Increment in Nu
300	1369.3	134.9	90.2	12.2	9.3	23.4
400	1526.3	149.5	90.2	13.0	9.9	23.4
500	1693.0	165.6	90.2	14.1	10.8	23.2
600	1919.9	185.1	90.4	16.5	12.3	25.2
700	2217.8	208.0	90.6	17.1	12.6	26.4

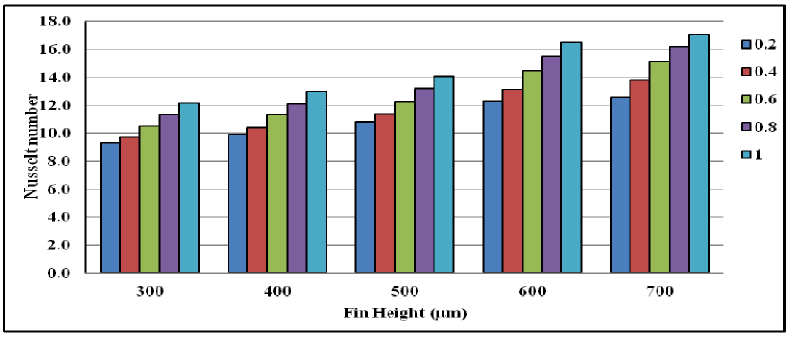

Figure 12: Nusselt Numbers for Different Fin Heights and Inlet Velocity of 0.2m/s to 1m/s

A very good quantity of unobstructed flow is observed in the channel on the leading edge side of the pin fins. Therefore in this region, the boundary layer is comparatively less disturbed. While the boundary layer disturbance produced due to flow diversion and flow separation created by the pin fin angle is comparatively higher on the other side. Thus, resulting in a very high convective heat transfer in the microchannel on the leading edge side of the pin fins compared to trailing end side. The streamline flow velocity pattern for microchannels with pin fin angle with the channel axis, changing from 10^o to 90^o is as shown in (Figure 14a-14e). These figures clearly show, how the flow separation due to the angle of the pin fin, effects the flow pattern in the channel. From a comparatively smoother flow at 10^o (Figure 14a), the flow separation goes on increasing till 40^o (Figure 14d). Further increase in the angle shows that the flow gets smoothen again, till 90^o. At 90^o angle, after flow separation i.e. the downstream side of the pin fin, the flow is observed to

recombining after passing around pin fin, making the flow smoother as shown in (Figure 14e).

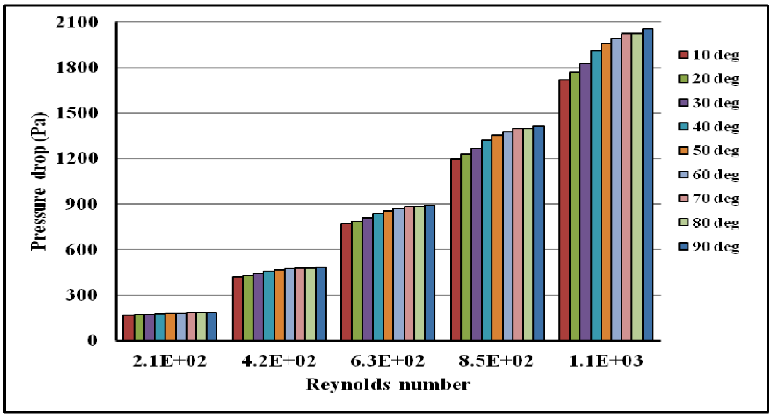

Figure 13: Variation of Pressure Drop with Reynolds Number

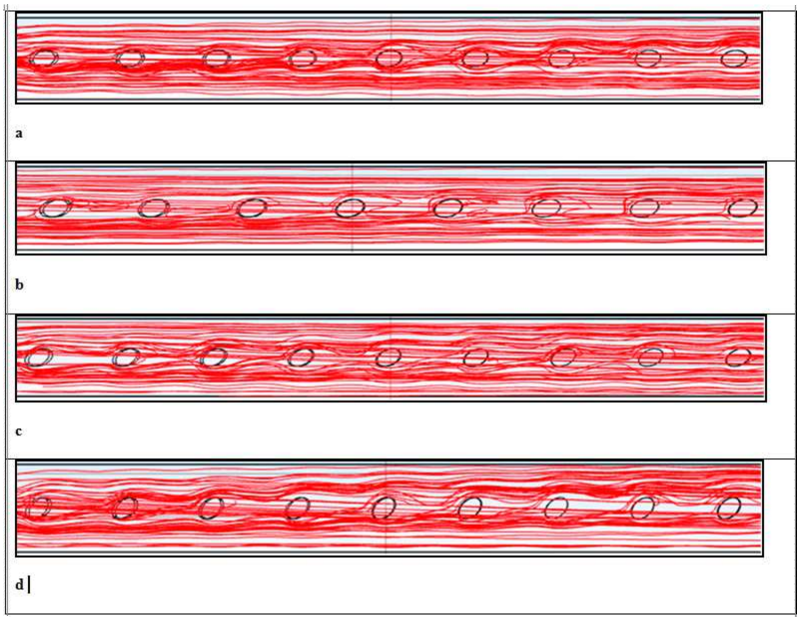

Figure 14: Streamline flow velocity pattern for a) 10^{o} b) 20^{o} c) 30^{o} d) 40^{o} e) 50^{o} f) 60^{o} g) 70^{o} h) 80^{o} i) 90^{o}

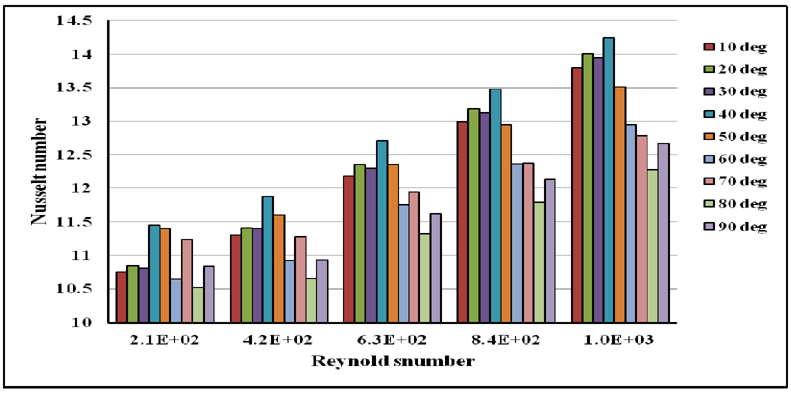

Figure 15: Variation of Nusselt Number with Reynolds Number

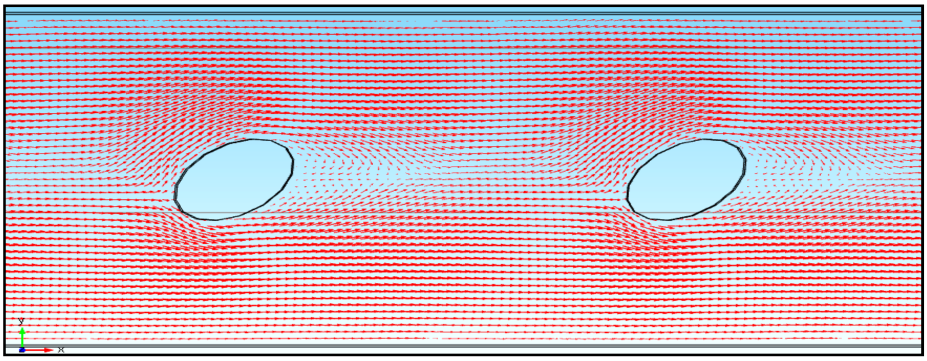

Figure 16: Arrow Flow Velocity Pattern a Microchannel with 40^{o} Pin Fin Angle with the Channel Axis.

The arrow flow velocity pattern for a microchannel with 40^{o} angle is as shown in (Figure 16). it is clear from the figure that the flow separation happens due to pin fin shape on the upstream side of the fin, while the flow is seen to form eddies during its recombining on the downstream side of the pin fin. Also, it is seen that the unobstructed flow is more on the side, where the upstream side of the fin is tilted towards the wall. The increment in the Nusselt number with the change in angle is more pronounced at lower angle values than that at higher angle values. Since the surface area of the pin fin is kept constant, the curve for variation of Fanning friction factor with Reynolds number remains similar to that of as shown in (Figure 6).

Analysis of Microchannel Having Elliptical Pin Fins and Pitch Varied

In this section, the microchannel with elliptical pin fins is analyzed for variable pitch, i.e. the distance between centers of two consecutive pin fins. The values of pitch considered for this study are from 800µm to1500µm. The location of the pin fins is along the channel central axis. The Pressure drop happening for the microchannel with different pitch values are as shown in (Figure 17) and it can be observed that the pressure drop increases with Reynolds number. The flow will experience separation after before every fin. This separated fluid flow tends to recombine after passing around the fin. This tendency of separation and recombination increases, as the pitch value increases. Therefore, the pressure drop increases with pitch value. The Nusselt number variation for the microchannel with varying pitch is as shown in (Figure 18). It can be seen from the figure that, 1300µm pitch distance gives comparatively better values of the Nusselt number when compared to other pitch values considered. The Nusselt number is seen to decrease for higher and lower values of pitch. The streamline velocity flow patterns for a lower value (800µm), a middle value (1200µm) and a higher pitch value (1500µm) are shown in (Figure19). From the figure, it is clear that, at comparatively lower pitch values, the scope for proper recombination of fluid is less. While at higher values of pitch, the fluid flows smoothly for a certain distance, after its recombination and before it gets separated due to next pin fin. This may result in lower values of the Nusselt number.

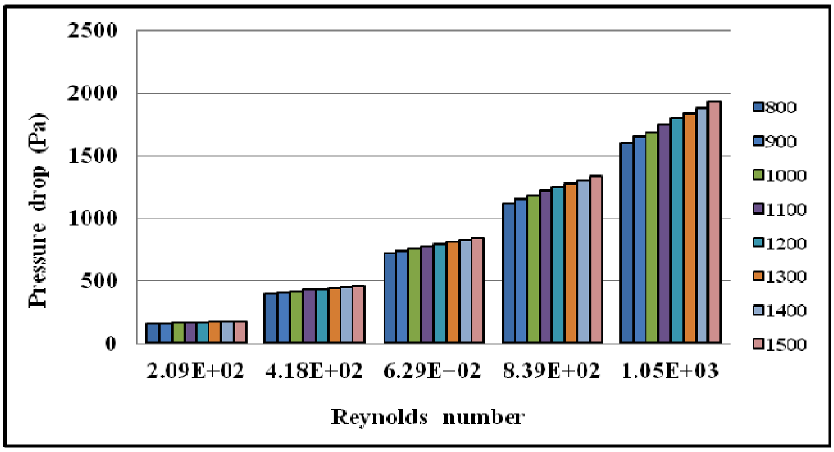

Figure 17: Variation of Pressure Drop in the Microchannel with Pitch Changed from 800µm to 1500µm

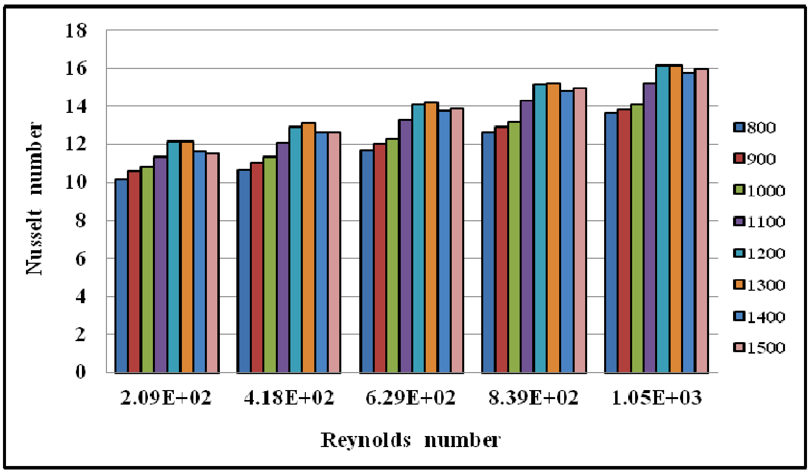

Figure 18: Variation of the Nusselt Number in the Microchannel with Pitch Changed from 800µm to 1500µm

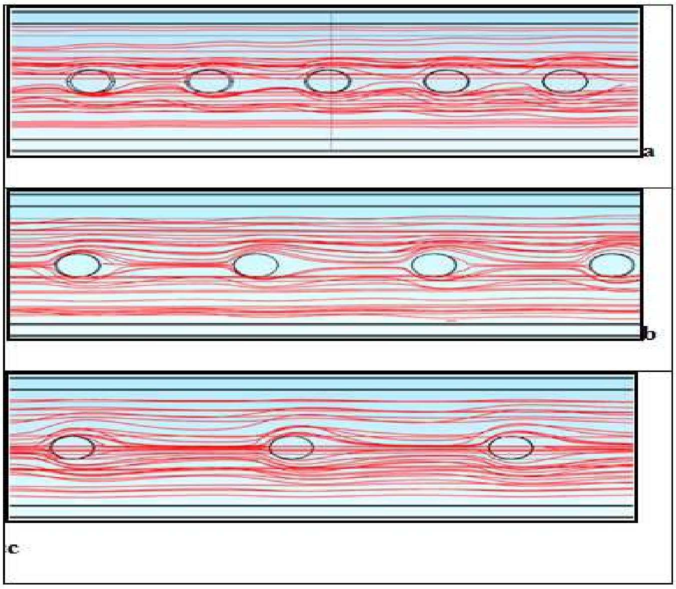

Figure 19: Streamline Velocity Profile for Different Pitch Values of a)800µm b)1200µm c)1500µm

CONCLUSIONS

Numerical analysis is carried out for a three-dimensional square microchannel with elliptical pin fins, for understanding the effect of pin fin geometry, pin fin height and the axial distance between the pin fins, in terms of Nusselt number and Pressure drop.

The following are the conclusions of this study.

- The pin fin shape in the microchannel, influence the microchannel performance. The square fin shows better thermal performance, while the elliptic pin fin offers minimum pressure drop.
- The angle of the major axis of the elliptical pin fin with the channel axis influence the microchannel thermal performance. The 40^{o} angle gives better results when compared to the other smaller and larger values of angle.
- The height of the pin fin also has a considerable effect on the microchannel performance. It is observed that the thermal performance increases with pin fin height, accompanied by an increased pressure drop penalty.
- The axial distance between the pin fins in the channel also effects the thermal performance of the microchannel considerably. 1300μm axial distance gave comparatively better results than other values considered in the study.

REFERENCES

1. *Tuckerman, D.B. and Pease, R. F. W. (1981), "High-performance heat sinking for VLSI," IEEE Electron device letters, Vol.2 (5), pp. 126–129.*
2. *Cheng, Y. J. (2007), "Numerical simulation of stacked microchannel heat sink with mixing-enhanced passive structure," International Communications in Heat and Mass Transfer," Vol. 34, pp. 295–303.*
3. *Jinliang, X., Yanxi, S., Wei, Z., Hua, Z. and Yunhua G. (2010), "Numerical simulations of interrupted and conventional microchannel heat sinks," International Journal of Heat and Mass Transfer, pp. 5906-5917.*
4. *John, T.J., Mathew, B. and Hegab, H. (2010), "Parametric study on the combined thermal and hydraulic performance of single phase micro pin-fin heat sinks part I: Square and circle geometries," International Journal of Thermal Sciences, Vol. 49, pp. 2177-2190.*
5. *Minghou, L., Dong, L., Sheng, X. and Yiliang, c. (2011), " Experimental study on liquid flow and heat transfer in a micro square pin-fin heat sink," International Journal for Heat Mass Transfer, Vol. 54, pp. 5602–5611.*
6. *Monoj B., Anupam D., and Mahanta, P. (2011), "Performance of Elliptical Pin Fin Heat Exchanger with Three Elliptical Perforations," CFD Letters, Vol. 3, pp. 65-73.*
7. *Carlos A. R., Satish, G. K., and Abel, H. (2013), " Performance of Online and Offset Micro Pin-Fin Heat Sinks With Variable Fin Density," IEEE Transactions on Components, Packaging and Manufacturing Technology, Vol. 3, PP. 86-93.*
8. *Tullius, J. F. Tullius, T. K. and Bayazitoglu, Y. (2012), " Optimization of short micro pin fins in minichannels," International Journal of Heat and Mass Transfer, Vol. 55, pp. 3921-3932.*
9. *Chiu, H.C., Hsieh, R. H. and Jang, J. H. (2013), "Numerical Analysis of the Heat Transfer of Heat sink with Micro-Pin-Fins," Vol. 52, pp. 759-764.*
10. *Haleh, S., Omid A., Khosrow J. and Goodarz A. (2013), " Numerical study of heat transfer performance of single-phase heat sinks with micro pin-fin structures," Applied Thermal Engineering, Vol. 58, pp. 68-76.*

11. Saad A.J., Wajahat A., Hafiz M. A.and Aysha M. A. (2014), "Applied Thermal Engineering", Vol.64, pp. 76-82.

12. Tzer, M. J. and Sheng, C. T. (2015)," Numerical Simulation of Laminar Forced Convection of Pin-Fin Heat Sink Array in a Channel by Using Porous Approach," Applied Sciences, Vol. 5, pp. 1846-1868.

13. Hafiz M. A. and Adrian B.,"A semi-empirical model for free-convection condensation on a horizontal pin–fin tubes," International Journal of Heat and Mass Transfer, Vol. 81, pp. 157–166.

14. Türker. İ., Mustafa, K. and Ali K. (2015), " The Effect of Micro Pin-Fin Shape on Thermal and Hydraulic Performance of Micro Pin-Fin Heat Sinks," Journal of Heat Transfer Engineering, Vol. 36, pp. 1447-1457.

15. Jin, Z., Shanbo, H., Liang, G., and Zhaoqin, H. (2016), "Numerical study and optimizing on a micro square pin-fin heat sink for electronic cooling," Applied Thermal Engineering, Vol. 93, pp. 1347-1359.

16. Kirsch, K. L. and Thol, K. A.,(2017), " Pressure loss and heat transfer performance for additively and conventionally manufactured pin fin arrays," International Journal of Heat and Mass Transfer, Vol. 108, pp. 2502-2513.

17. Aysha M. S., Waqas A., Hafiz M. A. Muzaffar A. and Muhammad A. N. (2017)," Evaluation of Nanofluids Performance for Simulated Microprocessor," Thermal Science, Vol. 21(5), pp. 2227-2236.